DOI 10.5012/bkcs.2011.32.2.681

Size-sorting of Micron-sized Particles using Two Gravitational SPLITT Fractionation (GSF) Connected in a Series (Tandem GSF)

Min Hyuk Kwon,[a] Yoon Jung Moon,[a] Euo Chang Jung,[†] Kyou Ho Lee,[‡] and Seungho Lee[*]

Separation Sciences Laboratory, Department of Chemistry, Hannam University, Daejeon 305-811, Korea [*]E-mail: slee@hnu.kr
[†]Korea Atomic Energy Research Institute, Daejeon 305-353, Korea
[‡]Department of Information and Communications Engineering, Inje University, Kimhe 621-749, Korea
Received October 8, 2010, Accepted December 22, 2010

SPLITT Fractionation (SF) provides separation of sample into two subpopulations. Separation into more than two subpopulations requires repeated SF operations. In this study, two Gravitation SF (GSF) channels were connected in a series (Tandem GSF) to obtain a separation into three subpopulations and to improve the fractionation efficiency (*FE*) of the fraction-*b* in the full-feed depletion (FFD) mode. In a single channel FFD-GSF operation, the fraction-*a* contained mostly the beads smaller than the cutoff diameter (d_c), while the fraction-*b* contained beads smaller than d_c as well as those larger than d_c, as expected. The measured *FE*'s of the fraction-*b* are much lower than those of the fraction-*a* in all cases. The *FE*'s of the fraction-*a* are higher than 84% with the average of about 91%, while those of the fraction-*b* are lower than 60% with the average of about 43%. No particular trends were found between *FE* and d_c, indicating the performance of FFD-GSF does not change with d_c in the range where tested. Also no clear trends were observed between the *FE* and the sample-feeding flow rate, indicating higher sample-feeding rate can be used to increase the sample throughput without losing resolution. When two GSF channels were connected so that the flow stream emerging from the outlet-*b* of the channel-1 is fed directly into the channel-2, all three *FE*'s measured for the fraction-1*a* were high with the average value of 99%, indicating it contains almost purely the beads smaller than d_c. The *FE*'s measured for the fraction-2*a* are still good with the average value of 92%. The *FE*'s measured for the fraction-2*b* are 64% in average, which is about 20% improvement from those obtained in a single channel FFD-GSF at the same conditions.

Key Words: SPLITT fractionation (SF), Tandem SF, Full-feed depletion (FFD) mode, Polyurethane

Introduction

SPLITT fractionation (SF) is a separation technique which has been proved to be useful for separation of macromolecules and colloidal particles.[1-5] SF provides a binary separation of a sample at a specific cutoff diameter (d_c). SF is thus useful for fractionation of various particulate samples having broad size distributions into fractions with narrower size distributions.[2,6-18]

Unlike most other separation techniques, which is operated in a batch mode (injection of a finite amount of sample), SF operates *via* a continuous feeding of the sample, thus providing separation in a preparative scale.[2,7,8,19] SF has a well-constructed theoretical basis and thus d_c can be easily controlled by adjusting the flow rates or if necessary the applied field strength.[20,21]

Conventionally SF is carried out in a thin, empty rectangular channel equipped with two splitters at both the inlet and outlet of the channel. Figure 1 shows a schematic view of a gravitational SF (GSF) channel, where the Earth's gravity is used as the external field. The sample (usually in a suspended form) is continuously fed through the inlet-*a*' while the carrier stream enters through the inlet-*b*'. The carrier flow rate is usually much higher than the sample-feeding flow rate, and, as a result, the inlet-splitting plane (ISP) is formed near the top of the channel. Particles leaving the inlet-splitter are immediately pushed above the ISP, and begin their migration toward the end of the channel. While migrating down the channel, particles settle down by gravity. Particles that settle down fast enough to cross the outlet splitting plane (OSP) will exit through the outlet-*b*, while the rest emerge from the upper outlet-*a*. Eventually, the fractions collected from the outlet-*a* and *b* contain particles smaller and

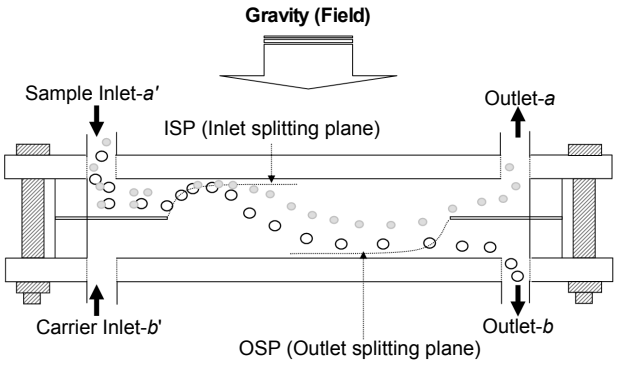

Figure 1. Schematic view of a conventional GSF channel.

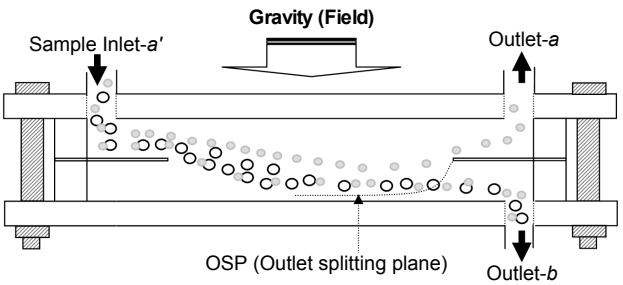

Figure 2. Schematic view of full-feed depletion (FFD) mode of GSF.

[a]These authors are equally distributed to this work.

larger than a certain diameter (the 'cut-off diameter', d_c), respectively. The lateral position of the OSP is determined by the ratio of the flow rates at the outlet-*a* to *b*, and thus d_c can be easily adjusted by controlling the outlet flow rates.

In the full-feed depletion (FFD) mode of GSF (FFD-GSF), the inlet-*b*' is closed (see Figure 2) and there is no feeding of the carrier liquid through the inlet-*b*' (only the OSP is established).[3] There exist no ISP, and the sample particles start settling down as soon as they enter the channel. Although the FFD mode of GSF suffers from a lack of resolution, as compared to the conventional mode (Figure 1), it allows an increase in the sample throughput (TP) and prevents the sample dilution.[3,18,22]

SF provides separation of sample into two fractions. In this study, two FFD-GSF channels were connected on-line, so that the sample can be separated into three fractions instead of two.[1]

Theory

In the conventional mode of GSF, the fraction of particles recovered from the outlet-*b*, F_b is given by[2]

$$F_b = \frac{\Delta V - V(a')}{V(a')} - \frac{V(a)}{V(a')} \tag{1}$$

where $V(a')$ and $V(a)$ are the flow rate entering the inlet-*a* and exiting the outlet-*b*, respectively. ΔV is the volumetric flow elements crossed by a particle during its transport in the GSF channel, which is given by[2]

$$\Delta V = b L U \tag{2}$$

where *b* and *L* are the breadth and the length of the channel, respectively, and *U* is the settling velocity of a particle. It can be seen from Eq. (1) that, with $V(a')$ held constant, F_b is inversely proportional to $V(a)$. The cutoff diameter d_c is defined as the diameter at which 50% of the particles exit outlet-*b* ($F_b = 0.5$), and is given by[2,8]

$$d_c = \sqrt{\frac{18\,\eta}{b\,L\,G\,\Delta\rho}\left(V(a) - 0.5V(a')\right)} \tag{3}$$

where η is the carrier viscosity, *G* the gravitational acceleration, $\Delta\rho$ the density difference between the carrier liquid and the particles.

In the FFD mode of GSF (FFD-GSF), the expression for d_c is slightly different from that of the conventional mode, and is given by[3,18,22]

$$d_c = \sqrt{\frac{18\,\eta}{b\,L\,G\,\Delta\rho}\left(V(a') - 0.5V(b)\right)} \tag{4}$$

In practical operations of FFD-GSF, $V(b)$ is determined by Eq. (4) for a given $V(a')$ once d_c is fixed.

In the FFD mode, the fraction-*a* is expected to contain only those particles having diameters equal to or smaller than d_c. However the fraction-*b* likely contains particles having diameters smaller than d_c as well as those larger than d_c. A reprocessing of the fraction-*b* is needed in order to increase the recovery yield of the particles with $d < d_c$ through the outlet-*a*.[3]

Still, the FFD mode of GSF provides some advantages over the conventional mode. In the FFD mode, because no inlet splitter is used, the inlet-flow (sample-feeding flow) of the channel is hydrodynamically stable, and thus higher sample concentration can be used. This will allow higher sample-throughput (the amount of sample that can be processed in a given time period). The operation of FFD mode is much simpler than the conventional mode because only one pump is needed. Also the sample is not diluted in the FFD mode as there is no feeding of the carrier liquid.

In this study, the fractionation efficiency (*FE*) of GSF was determined for the SF fraction-*a* and *b*, respectively, by[2]

$$FE \text{ for SF fraction - } a = \frac{\text{number of particles smaller than } d_c \text{ in fraction - } a}{\text{total number of particles measured}} \times 100 \tag{5}$$

$$FE \text{ for SF fraction - } b = \frac{\text{number of particles larger than } d_c \text{ in fraction - } b}{\text{total number of particles measured}} \times 100 \tag{6}$$

Experimental Section

Sample Preparation. The polyurethane (PU) beads having the density of 1.14 g mL^{-1} were mass-produced for industrial applications. They were dispersed at the concentration of 0.1% (w/v) in water containing 0.1% FL-70 (Fisher Scientific, Fait Lawn, NJ, USA) and 0.02% NaN_3, used as a bactericide.

Gravitational SPLITT Fractionation (GSF). Two GSF channels (named 'channel-1' and 'channel-2') were connected in a series for tandem GSF operations in this study. The channel-1 has the breadth, length, and the thickness of 3 cm, 20 cm, and 405 μm, respectively. The channel-2 has the same dimensions as the channel-1, except that the breadth is wider at 4 cm. A Gilson Minipuls 3 peristaltic pump (Gilson Medical Electronics, Middleton, WI, USA) provided the sample-feeding flow through the inlet-*a* of the channel-1 in all single channel or tandem FFD-GSF operations. The sample concentration was 0.1% dispersed in the carrier liquid, which was an aqueous solution of 0.1% (w/v) FL-70 (Fisher Scientific, Fair Lawn, NJ, USA) and 0.02% (w/v) sodium azide (NaN_3). The GSF system was maintained at room temperature at all times.

Optical Microscopy (OM). The optical microscopy (OM) was performed by using an Olympus BX51TF optical microscopy (Shinjuku Monolith, Shinjuku-ku, JAPAN). For all OM analysis of the particles, 500 ~ 1,000 beads were measured by using the Image Inside software (Focus, Daejeon, Korea).

Results and Discussion

Figure 3 shows OM pictures of the polyurethane (PU) beads (A) and those in the GSF fraction-*a* (B) and in the fraction-*b* (C)

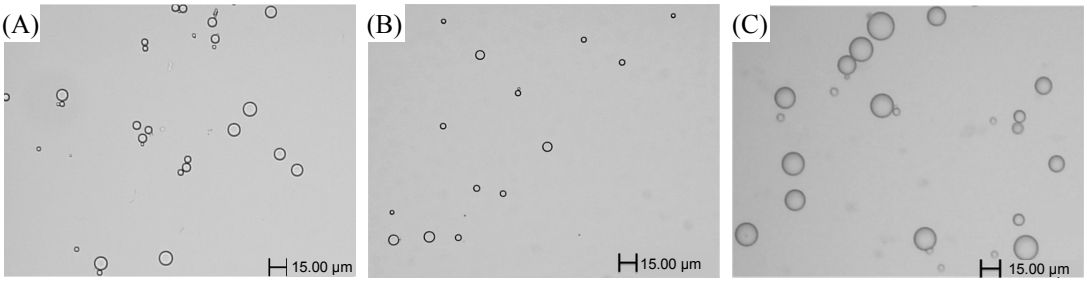

Figure 3. OM photographs of PU beads in the feeding sample (A) and those in the FFD-SF fraction-*a* (B) and *b* (C). d_c was set at 15 μm. The sample concentration was 0.1% and the sample-feeding flow rate ($V(a')$),$V(a)$ and $V(b)$ were 7.00, 6.17 and 0.83 mL/min, respectively.

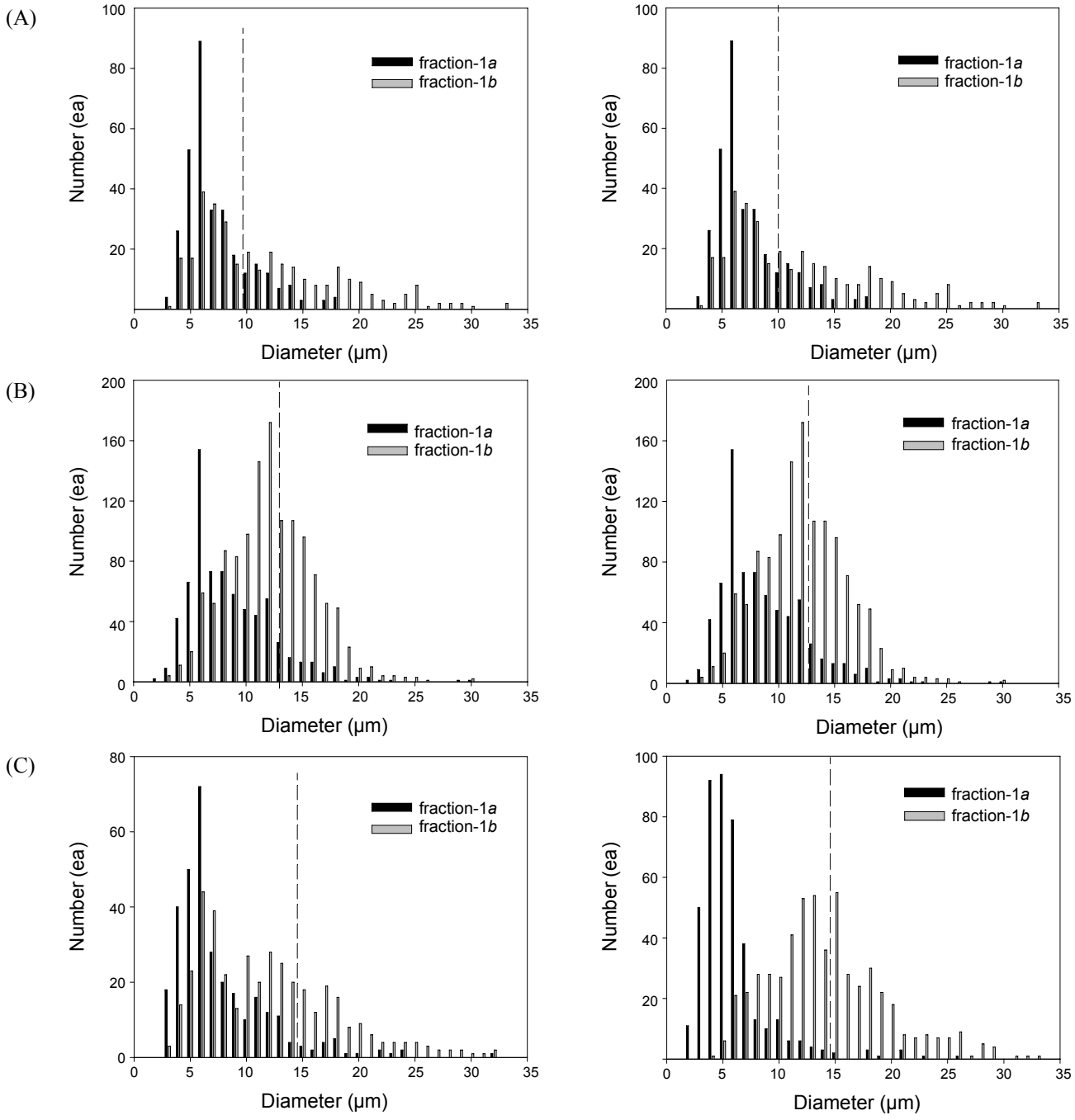

Figure 4. OM size distributions of PU beads in GSF-fractions obtained by single channel FFD-GSF operations using channel-1 at various conditions: (A) d_c = 10μm, sample-feeding = 3 (left) and 7 (right) mL/min; (B) d_c = 13μm, sample-feeding = 5 (left) and 11 (right) mL/min; (C) d_c = 15μm, sample-feeding = 7 (left) and 15 (right) mL/min.

Table 1. Experimental conditions and fractionation efficiencies (*FE*) measured for GSF-fractions shown in Figure 4

d_c (μm)	Flow rate (mL/min)			*FE* (%)	
	Sample-feeding	V_a	V_b	Fraction-*a*	Fraction-*b*
10	3	2.74	0.26	93	31
	7	2.74	4.26	89	60
13	5	4.64	0.36	84	53
	11	4.64	6.36	94	30
15	7	6.17	0.83	98	43
	15	6.17	8.83	90	43
			Average	91	43

obtained by a single channel FFD-GSF operation using the channel-1. d_c was set at 15 μm. The sample-feeding flow rate was 7 mL/min and $V(a)$ and $V(b)$ were 6.17 and 0.83 mL/min, respectively. It can be seen from Figure 3 that the PU sample has a broad size distribution ranging in diameter from about 2 to 30 μm. The fraction-*a* contains mostly the beads smaller than d_c, while the fraction-*b* contains beads smaller than d_c as well as those larger than d_c. This is characteristic of the FFD mode as explained earlier.

Figure 4 shows OM size distributions of PU beads in GSF-fractions obtained by single channel FFD-GSF operations using the channel-1 at various d_c and sample-feeding flow rates. In Figure 4(A), 4(B) and 4(C), d_c was set at 10, 13, and 15 μm, respectively. Two different sample-feeding flow rates were employed for each d_c, which was 3 and 7, 5 and 11, and 7 and 15 mL/min in the left and right plot of Figure 4(A), 4(B), and 4(C), respectively.

The experimental conditions and the *FE*'s measured for the GSF-fractions shown in Figure 4 are summarized in Table 1. As mentioned earlier, it is likely that the fraction-*b* obtained from the FFD mode of SF contains the particles with diameters smaller than d_c, causing *FE* of the fraction-*b* lower than that of the fraction-*a*. As expected, *FE*'s of the fraction-*b* are much lower than those of the fraction-*a* in all cases. The *FE*'s of the fraction-*a* were higher than 84%, while those of the fraction-*b* were lower than 60%. The *FE* does not show any dependency on d_c, indicating the performance of GSF does not change with d_c in the range where the system was tested.

With d_c set at 10 μm, the *FE* of the fraction-*a* was reduced slightly from 93 to 89% when the sample-feeding flow rate was increased from 3 to 7 mL/min. At the same time, *FE* of the fraction-*b* was greatly increased from 31 to 60%. With d_c set at 13 μm, *FE* of the fraction-*a* was increased from 84 to 94% when the sample-feeding flow rate was increased from 5 to 11 mL/min, while that of the fraction-*b* was reduced from 53 to 30%. With d_c set at 15 μm, *FE* of the fraction-*a* was decreased from 98 down to 90% when the sample-feeding flow rate was increased from 7 to 15 mL/min, while that of the fraction-*b* did not change. Relatively larger variation in *FE* of the fraction-*b* found at d_c = 10 or 13 μm may be due to V_b (the flow rate exiting through the outlet-*b*) being too low (lower than 0.5 mL/min), at which it is difficult to maintain the flow rate steady. No clear trends were observed between the *FE* and the sample-feeding flow rate, indicating higher sample-feeding rate can be used to increase the sample throughput without losing resolution. Results suggest one needs to find an optimum flow rates through preliminary testes.

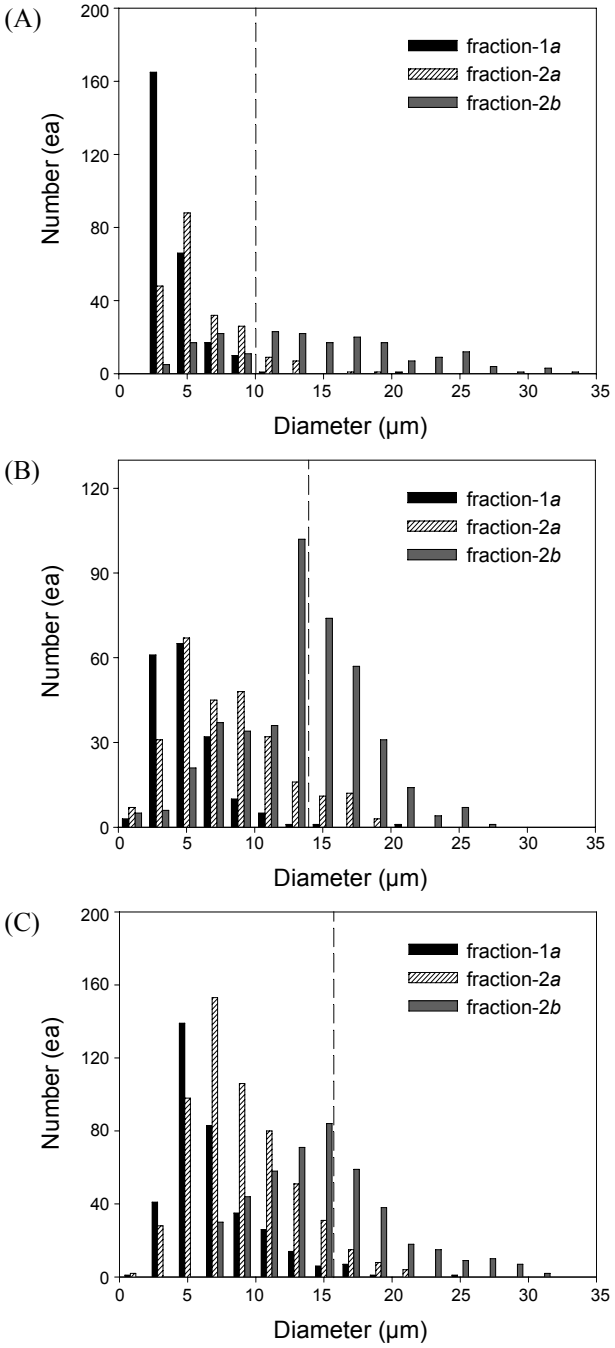

Figure 5. OM size distributions of PU beads in GSF-fractions obtained by Tandem FFD-GSF operations at various conditions: (A) d_c = 10 μm, sample-feeding = 7 mL/min; (B) d_c = 13 μm, sample-feeding = 11 mL/min; (C) d_c = 15μm, sample-feeding = 15 mL/min.

Figure 5 shows OM size distributions of PU beads in GSF fractions obtained by GSF/GSF operations at various conditions. Two GSF channels were connected so that the flow stream emerging from the outlet-*b* of the channel-1 is fed continuously into the channel-2 through the inlet-*a*. The experimental conditions and the *FE*'s measured for the GSF-fractions shown

Table 2. Experimental conditions and fractionation efficiencies (FE) measured for GSF-fractions shown in Figure 5

d_c (μm)	Flow rate (mL/min)				*FE* (%)		
	Sample-feeding	V_{1a}	V_{2a}	V_{2b}	Fraction-1*a*	Fraction-2*a*	Fraction-2*b*
10	7	2.74	3.66	0.60	100	93	76
13	11	4.64	6.18	0.18	99	90	64
15	15	6.17	8.23	0.60	98	94	52
		Average		99	92	64	

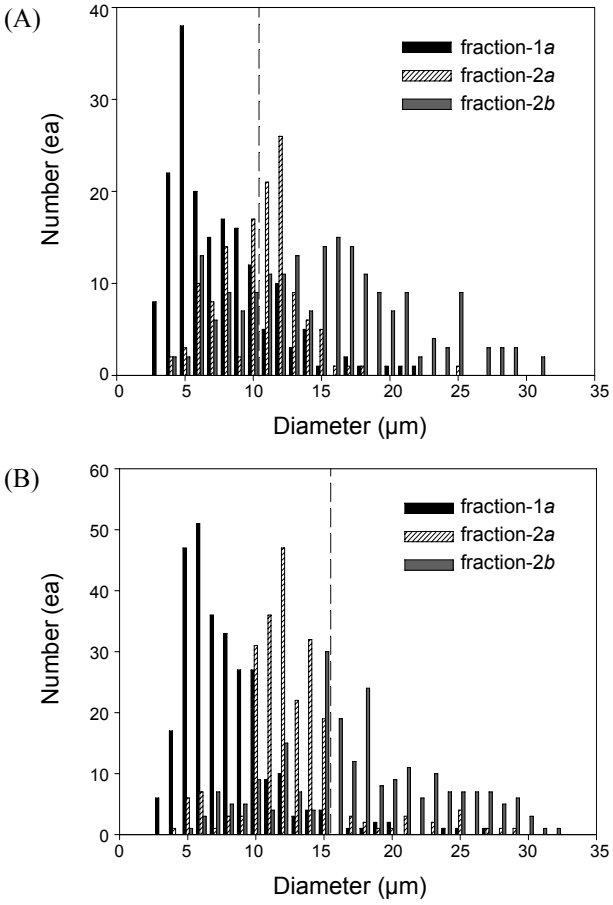

Figure 6. OM size distributions of PU beads in GSF-fractions obtained by Tandem FFD-GSF operations with channel-1 connected before (A) and after (B) channel-2. The sample-feeding flow rate was the same at 12 mL/min, and d_c was set at 10 and 15 μm for the first and the second channel, respectively.

in Figure 5 are summarized in Table 2, where V_{1a}, V_{2a} and V_{2b} are the flow rates emerging from the outlet-*a* of the channel-1, the outlet-*a* of the channel-2, and the outlet-*b* of the channel-2, respectively. Three fractions were collected in total which are 'fraction-1*a*' (fraction collected from the outlet-*a* of the channel-1), 'fraction-2*a*'(fraction collected from the outlet-*a* of the channel-2) and 'fraction-2*b*'(fraction collected from the outlet-*a* of the channel-2). In Figure 5(A), 5(B) and 5(C), d_c was set at 10, 13, and 15 μm, for both the channel-1 and channel-2, and the sample-feeding flow rate was 7, 11, and 15 mL/min, respectively.

It can be seen in Table 2 that all three *FE*'s measured for the fraction-1*a* are excellent with the average value of 98.6%, indicating all three fraction-*a*'s contain almost purely the beads smaller than d_c. The *FE*'s measured for the fraction-2*a* are still good with the average value of 92.3%, which are comparable with those obtained in Figure 4 at the same conditions (d_c and the sample-feeding flow rates). It is also seen in Table 2 that the *FE*'s measured for the fraction-2*b* are 64.2% in average, which were much improved from those obtained in Figure 4 at the same conditions. The results shown in Table 2 state that the GSF operation with two GSF channels connected in a series (GSF/GSF) provides much improved performance than a single GSF operation.

Table 3. Experimental conditions and fractionation efficiencies (FE) measured for SF-fractions shown in Figure 6

Channel connection	Flow rate (mL/min)			*FE* (%)		
	V_{1a}	V_{2a}	V_{2b}	Fraction-1*a*	Fraction-2*a*	Fraction-2*b*
channel-1/ channel-2	2.74	8.23	1.03	84	82	74
channel-2/ channel-1	3.66	6.17	2.17	83	66	56

Figure 6 shows OM size distributions of PU beads in GSF fractions obtained by two GSF/GSF operations with the channel-1 connected before (Figure 6(A)) and after (Figure 6(B)) the channel-2. This time, d_c's were set differently for the first and the second channel. In both Figure 6(A) and 6(B), d_c was set at 10 and 15 μm for the first channel ($d_{c,1}$) and the second channel ($d_{c,2}$), respectively. The sample-feeding flow rate was the same at 12 mL/min. The experimental conditions and the *FE*'s measured for the GSF-fractions shown in Figure 6 are summarized in Table 3. It can be seen in Table 3 that the *FE*'s measured for the fraction-1*a* are similar at around 83%, while the *FE*'s measured for the farction-2*a* and 2*b* are higher when the channel-1 was connected before the channel-2. The only difference between two channels is that the breadth of the channel-2 is 4 cm, which is wider than the channel-1 by 1 cm. It is interesting that *FE* changes by changing the order that the two channels of slightly different dimensions were connected by. However it is clear that the performance of GSF/GSF may change with the order that the GSF channels were connected by.

Conclusions

Results suggest that the tandem FFD-GSF operation provides improved performance than single channel FFD-GSF operation. For the fraction-*b*, the fractionation efficiency (*FE*) was improved by about 20%. *FE* is expected to be improved more if more channels are connected in a series. More work is planned to test the suggested method for real samples, and to develop theoretical interpretation for samples of inhomogeneous mixtures in density and shape.

Acknowledgments. Authors acknowledge support from Hannam University. This work was also supported by the nuclear research and development program through the National Re-

search Foundation of Korea funded by the Ministry of Education, Science and Technology.

References

1. Giddings, J. C. *Sep. Sci. Technol.* **1985**, *20*, 749.
2. Springston, S. R.; Myers, M. N.; Calvin Giddings, J. C. *Anal. Chem.* **1987**, *59*, 344.
3. Contado, C.; Dondi, F.; Beckett, R.; Giddings, J. C. *Anal. Chimica Acta* **1997**, *345*, 99.
4. Dondi, F.; Contado, C.; Blo, G.; Garçia Martin, S. *Chromatographia* **1998**, *48*, 643.
5. Contado, C.; Riello, F.; Blo, G.; Dondi, F. *J. of Chromatogr. A* **1999**, *845*, 303.
6. Giddings, J. C. *Sep. Sci. Technol.* **1988**, *23*, 931.
7. Levin, S.; Myers, M. N.; Giddings, J. C. *Sep. Sci. Technol.* **1989**, *24*, 1245.
8. Levin, S.; Giddings, J. C. *J. Chem. Tech. Biotechnol.* **1991**, *50*, 43.
9. Keil, R. G.; Tsamakis, E.; Fuh, C. B.; Giddings, J. C.; Hedges, J. I. *Geochimica et Cosmochimica Acta* **1994**, *58*, 879.
10. Zhang, J.; William, P. S.; Myers, M. N.; Giddings, J. C. *Sep. Sci. Technol.* **1994**, *29*, 2493.
11. Contado, C.; Reschiglian, P.; Faccini, S.; Zattoni, A.; Dondi, F. *J. of Chromatogr. A* **2000**, *871*, 449.
12. Contado, C.; Dondi, F. *Starch/Staerke* **2001**, *53*, 414.
13. Lee, S.; Park, H. Y.; Lee, S. K.; Yang, S. G.; Chul Hun, E. *Bull. Korean Chem. Soc.* **2001**, *22*, 616.
14. Moon, M. H.; Kang, D.; Lim, H.; Oh, J. E.; Chang, Y. S. *Environ. Sci. Technol.* **2002**, *36*, 4416.
15. Blo, G.; Conato, C.; Contado, C.; Fagioli, F.; Dondi, F. *Annali di Chimica* **2004**, *94*, 617.
16. Kim, W. S.; Park, M.; Lee, D. W.; Moon, M. H.; Lim, H.; Lee, S. *Anal. Bio. Chem.* **2004**, *378*, 746.
17. Moon, M. H.; Yang, S. G.; Lee, J. Y.; Lee, S. *Anal. Bio. Chem.* **2005**, *381*, 1299.
18. Lee, S.; Cho, S. K.; Yoon, J. W.; Choi, S. H.; Chun, J. H.; Eum, C. H.; Kwen, H. *J. Liq. Chromatogr. Related Technol.* **2010**, *33*, 27.
19. Giddings, J. C. *Sep. Sci. Technol.* **1988**, *23*, 119.
20. Contado, C.; Dondi, F. *J. Sep. Sci.* **2003**, *26*, 351.
21. Contado, C.; Hoyos, M. *Chromatographia* **2007**, *65*, 453.
22. Blo, G.; Contado, C.; Grandi, D.; Fagioli, F.; Dondi, F. *Anal. Chimica Acta* **2002**, *470*, 253.
23. Lee, S.; Lee, T. W.; Cho, S. K.; Kim, S. T.; Kang, D. Y.; Kwen, H.; Lee, S. K.; Eum, C. H. *Microchemical Journal* **2010**, *95*, 11.